Original Research Article

J. Funct. Mater. Biomol. 2(1)-2018 pp 25-30

SACRED HEART RESEARCH PUBLICATIONS

Journal of Functional Materials and Biomolecules

Journal homepage: www.shcpub.edu.in

ISSN: 2456-9429

Influence of rare earth (La^{3+}) substitution on Zinc ferrite Nanocrystals

S. Deepapriya [1], P. Annie Vinosha [1], John.D.Rodney [1], S.Krishnan [2], J. Ermine Jose [3], S. Jerome Das [1,]*

Received on 11 Apr 2018, Accepted on 12 May 2018

Abstract

Nano ferrites shows its striking outlook with both scientific and technological significance in most promising pertinent applications such as, biosensors, magnetic separation and photo catalytic applications. In this investigation, the study was engrossed on the progression of group IV element of zinc ferrite tailored via co-precipitation method. On doping lanthanum ion in $ZnFe_2O_4$ appears to be a fruitful approach to apprehend better physical properties of the lattice, which can be conveniently used magnetic, optical, and electrical properties of the as-synthesized nanocrystals. XRD analysis elucidates the cubic phase formation and lattice parameter, whereas the FTIR spectrum reveals the absorption band between 4000-400 cm^{-1}confirmed the cation vibration of the spinel structure. TEM micrograph image depicts the surface morphology and particle pattern. UV-visible spectral analysis reveals the significance of optical properties and the band gap was found using Kubelka-Munk plot and further the magnetic behaviour was evaluated using a VSM, under an applied magnetic field of 10 kOe. The results shows that doping the lanthanum ion in $ZnFe_2O_4$ tend to decrease in saturation magnetization as well as in anisotropy due to theirenhancement of crystallite size andcation distribution.

Keywords: Lanthanum, Co-precipitation, VSM.

1 Introduction

In recent decades, spinel ferrites are being reported as the most fascinating magnetic oxides which are extensively used due to their weird magnetic, optical and electrical properties[1]. These properties engrossed in the progression of the technical significance due to their environmental applications in the preparation of gas sensors, microwave absorption, energy storage device, and magnetic recording[2]. Zinc ferrite is a softmagnet with high saturation magnetization, chemical stability and high magneto crystalline anisotropy, which varies with the nature of their charges and cation distribution among the two sub-lattices[3]. Various processing techniques have been adopted to synthesize lanthanum doped zinc ferrite and undoped zinc ferrites such as co-precipitation, sol gel, combustion, hydrothermal and microemulsion[4]. In this investigation,a facile co-precipitation technique was used owing to its cost effective and economically feasible, to prepare spinel ferrites at low temperaturesas it offers the rewards in excess than other route like reliant on particle size, uniform composition, high activity and free from contamination[5]. Zincferrite and zinc lanthanum ferrite are of ferromagnetic nature with spinel structure and has a curie temperature at 790 K[6]. Doping the parent zinc spinel ferrite with $La^{3+}$are becoming the promising flavors for the enhancement of electrical and magnetic properties and it leads to the structural disorder, lattice strain as compared to undopedzinc ferrite[7], The focus of the study is to investigate the relation between the magnetization and cation distribution of the lanthanum doped and undoped zinc ferrite in the two sub-lattice sites. In addition, energy dissipated by the as-synthesized nanocrystals has a dynamic saturation magnetization and anisotropy.

2 Experimental

The Merkchemicals used in this experiment were used without further purification. The stoichiometric ratio of $Zn(NO_3)_2.6H_2O$, $La(NO_3)_2.6H_2O$, $Fe(NO_3)_2.6H_2O$ were synthesised economically viable co-precipitation route. The solution was dissolved separately in 75 ml of double distilled water and stirred continuously to attain uniform homogeneity. The 2M of NaOH was added drop-wise until pH 8 was attained and this pH was maintained throughout the experiment.The admixed solution was stirred for 2 h at 80°C inorder to convert hydroxides to ferrites. The obtained precipitate was centrifuged twice with distilled water and once with ethanol inorder to remove nitrates and impurities present if any. The resultant precipitate was dried at 70°C for 17 h in a hot air oven. The resultant by-product was calcinated in a muffle furnace at 500°C for 3 h, to acquire the final product of $ZnLaFe_2O_4$ nanocrystals. The similar process was also followed to synthesize $ZnFe_2O_4$.

* Corresponding author e-mail: jeromedas.s@gmail.com

[1]Department of Physics, Loyola College, Chennai- 600 034, India
[2]Department of Physics, Ramakrishna Mission Vivekananda College, Chennai-600 004, India
[3]Loyola - ICAM College of Engineering and Technology, Loyola Campus, Chennai-600 034, India

3 Results and Discussion

3.1 Structural analysis

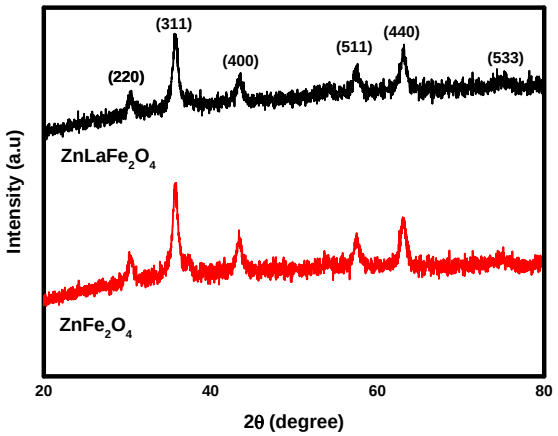

Figure 1 X-ray diffraction pattern of as-synthesised materials

The as-synthesized lanthanum doped zinc ferrite and un-doped zinc ferrite samples were analysed by X-ray diffraction pattern. The peaks depict the presence of crystalline size and phase purity of the nanocrystals. The relative intensity and positions of diffraction peaks at (220), (311), (400), (511), (440) and (533) corresponds to the phase formation of cubic spinel structure with Fd3m space group, which matches exceptionally well with the standard JCPDS file no. 39-1277 [8]. The presence of intense peak indicates the solubility of ions in their respective two sub-lattices with higher crystallinity, suggesting both doped and undoped zinc ferrites wereof polycrystalline in nature [9]. The excess substitution of La^{3+}ions tend to aggregate around the grain boundaries in the form of $ZnFe_2O_4$. Since the ionic radii of La^{3+} is higher than the Fe^{3+} ions, there existsthe replacement of Fe^{3+} ions[10]. Hence, the substitution of lanthanum ions persuades the structural distortion by increasing crystal imperfection owing to larger size and yields micro-strain[11]. Utilizing Scherrer equation, the Bragg angle (θ), diffraction peak width (311) at half of its height in radians (β) and D, the average size of crystallite for $ZnFe_2O_4$ and $ZnLaFe_2O_4$ of as-synthesized materials were calculated using the equation (1).

$$D = \frac{0.9\lambda}{\beta Cos\ \theta} \qquad (1)$$

Using the Bragg's equation the lattice constant 'a' for lanthanum doped and undoped zinc ferrite was calculated for the most prominent peak (311) by the following equation

$$a = d_{hkl}\sqrt{h^2 + k^2 + l^2} \qquad (2)$$

The lattice constant was used to determine the (hkl) miller indices of the plane for a known angle[12]. According to the Bragg's law, inter planar spacing was observed for the diffraction peaks. The X-ray density increases linearly with the doping of lanthanum in zinc ferrite is given by,

$$\rho_x = \frac{8M}{Na^3} \qquad (3)$$

where M is said to be molecular weight of as-synthesised material, a is the lattice constant, N the Avogadro's number. Hopping length in two sites ($L_A$and L_B) are known to be the distance between the magnetic ions, which are calculated by

$$L_A = 0.25a\sqrt{3} \qquad (4)$$

$$L_B = 0.25a\sqrt{2} \qquad (5)$$

The calculated values of L_A and L_B are shown in Table 1.It is found that the hopping length is directly proportional to the concentration of $La^{3+}$and the difference in the ionic radii of the constituent ions which explains the changes over doping of La^{3+} ion and increases the distance between the magnetic cations in $ZnFe_2O_4$ [13]. The lattice constant and X-ray density of the as-synthesised nanocrystal was tabulated.

Table 1 Geometric parameters of as-synthesized nanocrystals

Sample	Crystallite size (nm)	Lattice constant (Å)	L_A (kg/ m³)	L_B (kg/ m³)	ρ_x (gm/ cm³)
$ZnFe_2O_4$	9	8.342	3.574	2.882	5.2813
$ZnLaFe_2O_4$	11	8.371	3.596	2.894	5.5640

3.2 Interionic bond

Table 2 Parameters for Interionic sublattice

Interaction between sublattices	Interionic distance	Interionic bond angles
A-A	$d = \sqrt{3}\left(\frac{a}{4}\right)$	$\theta_5 = Cos^{-1}\left[\frac{r^2+q^2-d^2}{2rq}\right]$
B-B	$b = \sqrt{2}\left(\frac{a}{4}\right)$	$\theta_3 = Cos^{-1}\left[\frac{2p^2-d^2}{2p^2}\right]$
	$f = \sqrt{6}\left(\frac{a}{4}\right)$	$\theta_4 = Cos^{-1}\left[\frac{p^2+s^2-f^2}{2ps}\right]$
A-B	$c = \sqrt{11}\left(\frac{a}{8}\right)$	$\theta_2 = Cos^{-1}\left[\frac{p^2+r^2-e^2}{2pr}\right]$
	$e = \sqrt{3}\left(\frac{3a}{8}\right)$	$\theta_1 = Cos^{-1}\left[\frac{p^2+q^2-c^2}{2pq}\right]$
A-O	$q = a\sqrt{3}\left(u - \frac{1}{8}\right)$	
	$r = a\sqrt{11}\left(u - \frac{1}{8}\right)$	
B-O	$p = a\left(\frac{5}{8} - u\right)$	
	$s = a\sqrt{3}\left(\frac{1}{3u} + \frac{1}{8}\right)$	

The interionic distance between the bond lengths and bond angles of cations and anions show the magnetic interaction between the sub-lattice of the two sites namely octahedral and tetrahedral. The variation in the bond lengths and bond angles among the cation-cation (Me-Me) and cation-anion (Me-O) modifies theasset of the magnetic interactions in A-A, B-B and A-B sub lattices[14]. Octahedral and tetrahedral edges are calculated with help of expressions listed in Table 2

The magnetic interaction of A-site and B-site is aligned in the opposite direction with each other and it is comparatively stronger than the ions A-A and B-B. The substitution of lanthanum in $ZnFe_2O_4$ changes the cation distribution due to the different ionic radius which causes an increase or decrease in the bond angle and bond length, hence it enhance the magnetic properties of the ferrites[15]. Thecation (A-A),(B-B) and (A-B) and anion (A-O) (B-O) distance varies when the lanthanum is doped in $ZnFe_2O_4$, similarly the bond angles were found for cations among tetrahedral and octahedral sites for their ionic radii and values are tabulated.

Table 3 Interionic bond lengths and angles in $ZnFe_2O_4$ and $ZnLaFe_2O_4$

Content	$ZnFe_2O_4$	$ZnLaFe_2O_4$
b	2.8741	2.8945
c	3.5631	3.6201
d	3.6475	3.7210
e	4.8240	4.9625
f	5.6439	5.8472
p	2.4526	2.4632
q	1.6452	1.7216
r	2.8764	2.896
s	3.7251	3.7960
θ_1	131.62	131.74
θ_2	142.97	143.02
θ_3	93.741	93.856
θ_4	120.132	120.456
θ_5	103.452	103.64

3.3 TEM

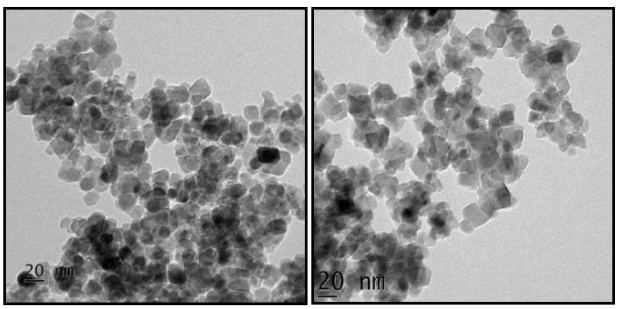

$ZnFe_2O_4$ $ZnLaFe_2O_4$

Figure 2 TEM micrograph of as-synthesised materials

Microstructure of lanthanum doped and undoped zinc ferrite exhibits an angular morphology and the dimension allocation was confirmed using Transmission Electron Microscope. The micrograph exhibits substantial agglomeration for as-synthesized nanocrystals owing to their incredible magnetic property and by the weak interaction of vanderwaals force [16].The as-synthesised material has a spinel structure perceived vital consideration owing to their electrical and magnetic properties (fig 2)

3.4 FTIR analysis

FTIR absorption spectra is used to inspect the presence of bond in the cation distribution and change in the spinel structure owing to their combination of distant ions which effects the lattice vibration [17]. The absorption spectrum is an significant tool to distinguish about the position of cation-anion in the crystal vibration modes. The FTIR spectra of lanthanum doped and undoped $ZnFe_2O_4$were chronicled in the range of 400 – 600 cm^{-1} are exposed in the fig 3. It is found that the spectra has a metal oxygen bond (υ_1) and (υ_2) due to their intrinsic vibrations of the A and B site[18]. The absorption band (υ_1), detected in the array of 576 cm^{-1} is ascribed to the tetrahedral site at low frequency and (υ_2) observed in the array of 402cm^{-1}at octahedral site in the high frequency band [19].

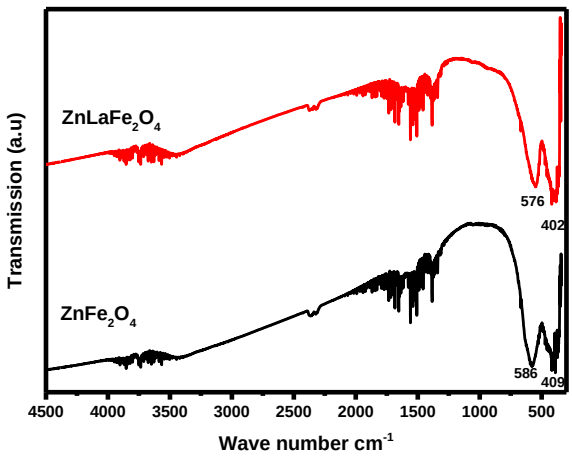

Figure 3 FTIR absorption spectrum of as-synthesized material

3.5 Uv- Analysis

The absorption spectra of the as-synthesized $ZnFe_2O_4$ and $ZnLaFe_2O_4$ nanomaterials (Fig 4) shows. The electronic transistion takes place when an electron takes a energy of photon and make a transistion to higher energy level from the lower energy level.Hence there is a photon shift towards higher wavelength due to the doping of La^{3+}ion with maximum absorption[20]. As a result of photon electron interaction, interface defects and points defects there is an inconsistency flanked by the absorbance band edge was observed. The band gap was

estimated by Kubelka-Munkplot and theband gap found to be (E_g= 2.24 eV for $ZnFe_2O_4$ and E_g= 2.12 eV for $ZnLaFe_2O_4$). The energy gap was subjective with increase and decreasing speck size due to the quantum confinement effect [21].

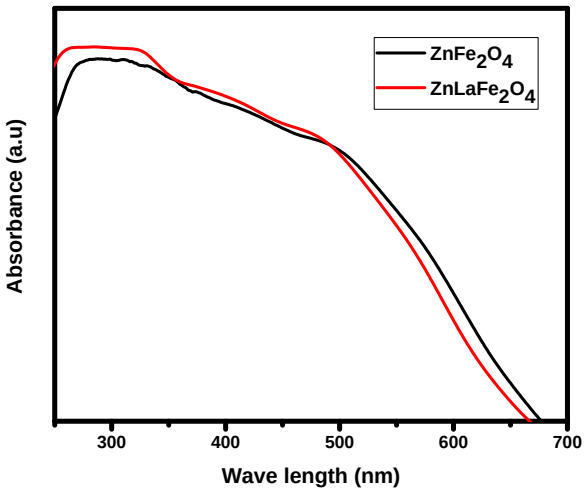

Figure 4 Uv –visible spectrum of as-synthesised materials

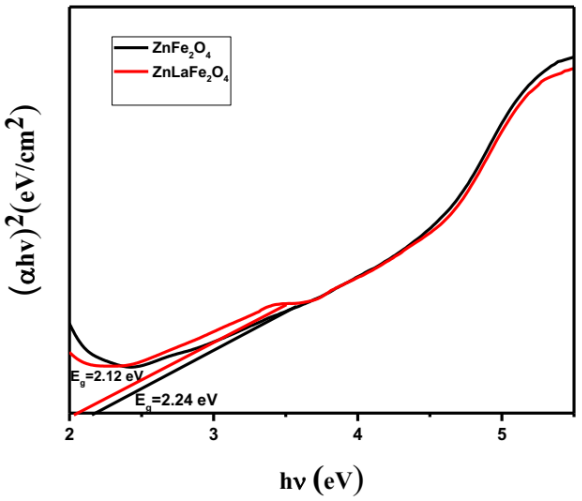

Figure 5 Bandgap of as-synthesized material.

3.6 VSM

The magnetic properties was deliberated in detail by vibrating sample magnetometer. The lanthanum doped and undoped zinc ferrite shows a definite hysteresis loop at ±10kOe as maximum applied field and it was notably narrow;for the reason that the nanoparticle with a small average diameter[22]. The as-synthesised nanocrystal exhibits magnetic property near to the ferromagnetic nature and the magnetization of lanthanum doped and un doped $ZnFe_2O_4$ rely on the high saturation, remnant magnetization, coercivity and the number of magnetic ions occupying the two interstitial sub-lattice. Hence, Fe^{3+} ions occupy octahedral site while Zn^{2+} prefers the tetrahedral site, whereas La^{3+} favors the octahedral site of the spinel lattice are known to be the main donors of magnetic properties [23]. The magnetization of the cation distribution is given by

$$(Fe^{3+})\left[Fe^{3+}_{1-x}Zn^{2+}La^{3+}_{x}\right]O^{2-}_{4} \qquad (6)$$

The saturation magnetization (Ms), corecivity (Hc), retentivity (Mr) values and magnetic moment of the synthesized $ZnFe_2O_4$ and $ZnLaFe_2O_4$ are listed in Table 4. The hysteresis curve specifies the ordering of ionic spin states and as-sythesisednanocomposite possesses a ferromagnetic nature [24]. The obtained saturation magnetization increases while coercivity decreases due to the domain formation

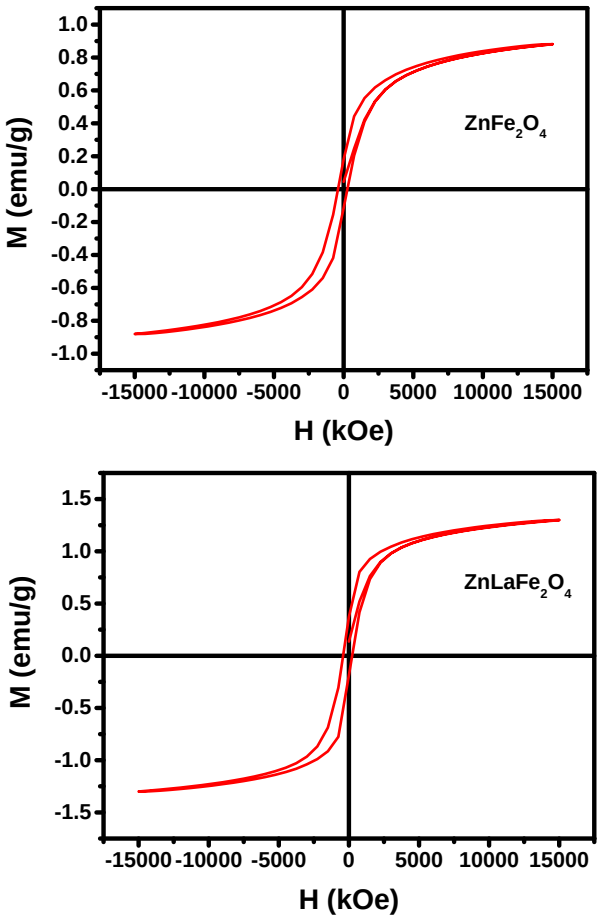

Figure 6 VSM of as-synthesised Materials

The dependence of magnetization near saturation is given by

$$M = M_s\left[1 - \frac{b}{H^2}\right] + kH \qquad (7)$$

where, M is the magnetization, M_s is saturation magnetization, $b = \frac{8}{105}\frac{k_1^2}{M_s^2\mu_o^2}$, K_1 is the cubic anisotropy constant, μ_o is the permeability of the free space, H is the applied magnetic field.

The following equations for the determination of cubic anisotropy constant, Bohr magneton and Initial permeability was given by
anisotropy constant

$$k_1 = \mu_0 M_s \sqrt{\frac{105b}{8}} \quad (8)$$

initial permeability

$$\mu_i = \frac{M_s^2 xD}{K} \quad (9)$$

Bohr magnetron

$$\mu_B = \frac{Mx\,M_s}{5585\,x\,\rho_{xray}} \quad (10)$$

The factors such as magneto crystalline anisotropy constant, initial permeability, and Bohr magneton of Zn^{3+}, La^{3+} and Fe^{3+} at A site, B site and surface spin effects are found to be dependent for the variations in magnetic properties in La doped Zn nanoferrites [25].

Table 4 Various parametersobtained in magnetic studies

Samples	M_s (emu/g)	M_r (emu/g)	Bohr Magneton	H_c (kOe)	Anisotropy constant	Initial permeability
$ZnFe_2O_4$	112.36	97.24	0.89	113.51	40657.55	106.74
$ZnLaFe_2O_4$	86.92	58.91	0.62	386.24	34970.89	65.89

4 Conclusions

In this paper, synthesis of $ZnFe_2O_4$ and $ZnLaFe_2O_4$were reported using a viable co-precipitation method. The crystallite size was determined around 9-11 nm and various parameters was calculated from XRD. By doping lanthanum ions, the impurity phase of the crystalline structure has been increased in the existence of the $ZnFe_2O_4$. FTIR spectrum confirms the functional group and elucidates that the bond length increases with the force constant of the as-synthesized material. The TEM micrographs depicts morphology of as-synthesized nanocrystals with agglomeration due to union of primary particles. In Uv-vis spectrum, found the bandgap for as-synthesised material in the range of 2.12 – 2.24 eV. The large variation in the magnetization was observed in VSM and it shows that ionic spin states has a ferromagnetic nature.

References

[1] P. M. Prithviraj Swamy, S. Basavaraja, A. Lagashetty, N. V. Srinivas Rao, R. Nijagunappa, and A. Venkataraman, "Synthesis and characterization of zinc ferrite nanoparticles obtained by self-propagating low-temperature combustion method," *Bull. Mater. Sci.*, vol. 34, no. 7, pp. 1325–1330, 2012.

[2] S. Patra and L. K. Singhal, "Materials Sciences and Applications," *Mater. Sci. Appl.*, vol. 4, no. 1, pp. 70–76, 2013.

[3] P. Tailhades *et al.*, "Cation Migration and Coercivity in Mixed Copper-Cobalt Spinel Ferrite Powders," *J. Solid State Chem.*, vol. 141, no. 1, pp. 56–63, 1998.

[4] S. Bera *et al.*, "Formation of zinc ferrite by solid-state reaction and its characterization by XRD and XPS," *J. Mater. Sci.*, vol. 36, no. 22, pp. 5379–5384, 2001.

[5] J. Kennedy, G. V. M. Williams, P. P. Murmu, and B. J. Ruck, "Intrinsic magnetic order and inhomogeneous transport in Gd-implanted zinc oxide," *Phys. Rev. B - Condens. Matter Mater. Phys.*, vol. 88, no. 21, pp. 1–5, 2013.

[6] S. Ayyappan, S. Mahadevan, P. Chandramohan, M. P. Srinivasan, J. Philip, and B. Raj, "Influence of Co $^{2+}$ Ion Concentration on the Size, Magnetic Properties, and Purity of CoFe $_2$ O $_4$ Spinel Ferrite Nanoparticles," *J. Phys. Chem. C*, vol. 114, no. 14, pp. 6334–6341, 2010.

[7] M. Siva Ram Prasad, B. B. V. S. V. Prasad, B. Rajesh, K. H. Rao, and K. V. Ramesh, "Magnetic properties and DC electrical resistivity studies on cadmium substituted nickelzinc ferrite system," *J. Magn. Magn. Mater.*, vol. 323, no. 16, pp. 2115–2121, 2011.

[8] M. Manivannan, S.A Martin Britto Dhas, and M.Jose Photoacoustic and dielectric spectroscopic studies of 4-dimethylamino-n-methyl-4-stilbazolium to stylate single crystal: An efficient tetrahertz emitter *J.Cryst.Growth* Vol.566. pp. 167-7 2016.

[9] J. D. Rodney *et al.*, "Photo-Fenton degradation of nano-structured La doped CuO nanoparticles synthesized by combustion technique," *Optik (Stuttg).*, 2018.

[10] M. Ishaque *et al.*, "Study on the electromagnetic behavior evaluation of Y3+doped cobalt nanocrystals synthesized via co-precipitation route," *J. Magn. Magn. Mater.*, vol. 372, pp. 68–73, 2014.

[11] Z. Karimi, Y. Mohammadifar, H. Shokrollahi, S. K. Asl, G. Yousefi, and L. Karimi, "Magnetic and structural properties of nano sized Dy-doped cobalt ferrite synthesized by co-precipitation," *J. Magn. Magn. Mater.*, vol. 361, pp. 150–156, 2014.

[12] M. Augustin and T. Balu, "Estimation of lattice stress and strain in zinc ferrite nanoparticles by williamson-hall and size-strain plot methods," pp. 13–17, 2015.

[13] L. C. Xue *et al.*, "Study of electron transition energies between anions and cations in spinel ferrites using differential UV-vis absorption spectra," *Phys. B Condens. Matter*, vol. 492, pp. 61–64, 2016.

[14] R. D. Shannon, "Revised effective ionic radii and systematic studies of interatomic distances in halides and chalcogenides," *Acta Crystallogr. Sect. A*, vol. 32, no. 5, pp. 751–767, 1976.

[15] S. Gyergyek, D. Makovec, A. Kodre, I. Arčon, M. Jagodič, and M. Drofenik, "Influence of synthesis method on structural and magnetic properties of

cobalt ferrite nanoparticles," *J. Nanoparticle Res.*, vol. 12, no. 4, pp. 1263–1273, 2010.

[16] P. C. Morais *et al.*, "Synthesis and characterization of size-controlled cobalt-ferrite-based ionic ferrofluids," *J. Magn. Magn. Mater.*, vol. 225, no. 1–2, pp. 37–40, 2001.

[17] A. B. Gadkari, T. J. Shinde, and P. N. Vasambekar, "Synthesis, characterization and magnetic properties of La3+added Mg-Cd ferrites prepared by oxalate co-precipitation method," *J. Alloys Compd.*, vol. 509, no. 3, pp. 966–972, 2011.

[18] C. G. Ramankutty and S. Sugunan, "Surface properties and catalytic activity of ferrospinels of nickel, cobalt and copper, prepared by soft chemical methods," *Appl. Catal., A*, vol. 218, pp. 39–51, 2001.

[19] R. Sharma *et al.*, "Improvement in magnetic behaviour of cobalt doped magnesium zinc nano-ferrites via co-precipitation route," *J. Alloys Compd.*, vol. 684, pp. 569–581, 2016.

[20] N. Bouhadouza, A. Rais, S. Kaoua, M. Moreau, K. Taibi, and A. Addou, "Structural and vibrational studies of NiAlxFe2-xO4ferrites (0≤x≤1)," *Ceram. Int.*, vol. 41, pp. 0–17, 2015.

[21] L. L. Lang *et al.*, "Study of the magnetic structure and the cation distributions in MnCo spinel ferrites," *Phys. B Condens. Matter*, vol. 462, pp. 47–53, 2015.

[22] K. K. Bamzai, G. Kour, B. Kaur, and S. D. Kulkarni, "Effect of cation distribution on structural and magnetic properties of Dy substituted magnesium ferrite," *J. Magn. Magn. Mater.*, vol. 327, pp. 159–166, 2013.

[23] W. Onreabroy, K. Papato, G. Rujijanagul, K. Pengpat, and T. Tunkasiri, "Study of strontium ferrites substituted by lanthanum on the structural and magnetic properties," *Ceram. Int.*, vol. 38, no. SUPPL. 1, pp. S415–S419, 2012.

[24] P. Kumar, S. K. Sharma, M. Knobel, J. Chand, and M. Singh, "Investigations of lanthanum doping on magnetic properties of nano cobalt ferrites," *J. Electroceramics*, vol. 27, no. 2, pp. 51–55, 2011.

[25] S. R. Naik and A. V. Salker, "Change in the magnetostructural properties of rare earth doped cobalt ferrites relative to the magnetic anisotropy," *J. Mater. Chem.*, vol. 22, no. 6, pp. 2740–2750, 2012.